0026-895X/96/050938-10$3.00/0

MOLECULAR PHARMACOLOGY, 49:938-947 (1996).

# Ability of Nondepolarizing Neuromuscular Blocking Drugs to Act as Partial Agonists at Fetal and Adult Mouse Muscle Nicotinic Receptors

GEORGE HAROLD FLETCHER and JOE HENRY STEINBACH

*Department of Anesthesiology, Washington University School of Medicine, St. Louis, Missouri 63110*

Received October 27, 1995; Accepted January 23, 1996

**SUMMARY**

We studied the ability of four nondepolarizing neuromuscular blocking agents (atracurium, gallamine, metocurine, and pancuronium) to act as competitive antagonists at mouse adult- and fetal-type muscle nicotinic receptors. Receptor subunits for the fetal-type ($\alpha$, $\beta$, $\gamma$, and $\delta$) and adult-type ($\alpha$, $\beta$, $\epsilon$, and $\delta$) receptors were stably expressed in quail fibroblasts. Binding for each drug was determined by the ability of the agents to reduce the initial rate of labeled $\alpha$-bungarotoxin binding, and functional consequences were determined with the use of voltage-clamp studies of their ability to elicit currents or to block currents elicited by acetylcholine. Each agent has a different affinity for the two acetylcholine-binding sites on a single receptor; the rank order of affinities is the same for both fetal- and adult-type receptors. All agents inhibited activation of adult-type receptors by ACh, consistent with the idea that occupation of either the high or low affinity site completely blocks activation when acetylcholine binds to the other site on the receptor. The concentration dependence of the inhibition of acetylcholine-elicited current was predictable from the affinities estimated from independent measurements of the inhibition of $\alpha$-bungarotoxin binding. Gallamine and pancuronium also acted as competitive inhibitors of fetal-type receptors, and, again, the concentration dependence of the inhibition was predictable from binding data. However, metocurine and atracurium could potentiate the responses of fetal-type receptors to low concentrations of acetylcholine. The interaction of metocurine and atracurium with acetylcholine at fetal-type receptors could be accounted for by a weak partial agonist activity. It has been suggested that some pairs of nondepolarizing neuromuscular blocking agents might be more efficacious because the high affinity site for one agent might be the low affinity site for another. This hypothesis was tested for the pair of agents metocurine and gallamine by determining the ability of a mixture of agents to inhibit the binding of $\alpha$-bungarotoxin. The results are consistent with the idea that both metocurine and gallamine have a high affinity for the same site on the receptor. The ability of gallamine to block the partial agonist action of metocurine at fetal-type receptors was tested as well and also indicated that both agents share the same high affinity site.

NDBs are frequently used during surgical procedures to produce relaxation and have also been used as pharmacological probes of the muscle nicotinic receptor (AChR). It is commonly accepted that the major mechanism of action is competitive inhibition of activation: the agent occupies the same site(s) on the AChR as ACh itself but does not activate the receptor and so prevents activation by ACh (1). As our understanding of the structure and function of the AChR has increased, however, so have the possible complexities in the mechanism of action of these drugs. It is clear that there are two sites on each receptor that bind ACh and that both sites must be occupied by ACh for there to be a high probability that the ion channel will open (for a review, see Ref. 2). NDBs also bind to two sites on each receptor and show distinct affinities for the two sites, which may differ by 100-fold (3, 4). Previous work has indicated that occupancy of a single site by a NDB essentially prevents activation of the AChR by ACh, even when ACh binds to the remaining free site (3). Therefore, the ability of an NDB to inhibit activation by ACh is largely determined by the affinity for the higher affinity binding site.

The nicotinic receptors found on skeletal muscle fibers are heteromultimers composed of five subunits. Each receptor contains two copies of the $\alpha$1 subunit and one copy each of the $\beta$1, $\delta$, and $\gamma$ or $\epsilon$ subunits. Two isoforms of muscle nicotinic receptor exist, which differ in the last subunit incorporated. In the fetal type, one copy of the $\gamma$ subunit is included, whereas in the adult type, the $\epsilon$ subunit occurs. The sites to

This research was supported by National Institutes of Health Grants PO1-GM47969 and RO1-NS22356 to J.H.S.

**ABBREVIATIONS:** NDB, nondepolarizing neuromuscular blocking agent; ACh, acetylcholine; AChR, acetylcholine receptor; I-BTX, iodinated $\alpha$-bungarotoxin; EGTA, ethylene glycol bis($\beta$-aminoethyl ether)-*N,N,N',N'*-tetraacetic acid; HEPES, 4-(2-hydroxyethyl)-1-piperazineethanesulfonic acid.

which ACh and NDBs bind are located at the $\alpha$-$\delta$ and $\alpha$-$\gamma/\epsilon$ interfaces (5, 6), with residues contained in each subunit contributing to the site (5, 7).

The prototypical NDB is *d*-tubocurarine (curare). Although curare reduces the response of fetal-type AChR to high concentrations of ACh, curare also serves as a very weak agonist at fetal-type AChR (8) and can actually enhance the response to low doses of ACh (9, 10). However, curare does not activate adult-type AChR (9, 10). Curare binds to fetal- and adult-type AChR with indistinguishable affinities (10, 11) but is unable to activate adult-type AChR.

We explored the ability of several structurally diverse NDBs to bind to and activate fetal- and adult-type mouse muscle nicotinic receptors. We used stably transfected fibroblasts that express either adult- or fetal-type receptors so functional assays (through measurement of voltage-clamped membrane currents) and binding assays (through measurement of the initial rate of $\alpha$-bungarotoxin binding) could be performed on the same preparation. All of the drugs used acted as competitive antagonists at the adult-type AChR, but two demonstrated weak partial agonist activity at fetal-type receptors.

## Materials and Methods

Unless otherwise noted, all chemicals were obtained from Sigma Chemical Co. (St. Louis, MO). I-BTX was prepared using the iodine monochloride method (12).

Quail fibroblasts (QT6 cells) were transfected with cDNAs coding for mouse muscle nicotinic receptor subunits and for neomycin resistance, and colonies with resistance to G418 were screened for the binding of I-BTX (9, 13). One line expressing the $\alpha 1$, $\beta 1$, $\gamma$, and $\delta$ subunits (fetal-type receptors, QF18 cells) and one line expressing $\alpha 1$, $\beta 1$, $\delta$, and $\epsilon$ subunits (adult-type receptors, QA33 cells) were used in these studies. The population was enriched for cells with a high surface density of receptors by adsorbing the cells to surfaces coated with an antibody to an extracellular region of the $\alpha 1$ subunit (monoclonal antibody 35; see Ref. 14), as described previously (15). Cells were maintained in Earle's Medium 199 supplemented with 10% (v/v) tryptose phosphate broth (GIBCO, Grand Island, NY), 5% fetal bovine serum (Hyclone, Logan, UT), 1% dimethylsulfoxide, 100 units/ml penicillin, and 100 $\mu$g/ml streptomycin.

The blocking agents used were gallamine triethiodide (Sigma), metocurine iodide (a gift from Dr. S. Sine, Mayo Clinic; originally supplied by Eli Lilly, Indianapolis IN), pancuronium bromide (Sigma), and atracurium besylate (supplied by Burroughs-Wellcome, Research Triangle Park, NC). Atracurium was dissolved in buffer at pH 3.5 to enhance stability of stock solutions, and working solutions were used within 4 hr of preparation. Other drugs were dissolved in recording saline (see below). Stocks were kept frozen and in the dark.

The binding of drugs was determined from the inhibition of the initial rate of I-BTX binding (10, 16). Dishes of cells were preincubated with a given concentration of NDB for 10 min; then, the solution was changed to one containing I-BTX (7.5 nM) and NDB for 5 min. The dish was then washed rapidly 4 times, and bound radioactivity was determined with a $\gamma$ counter. Nonspecific binding was determined by the addition of 1 $\mu$M unlabeled $\alpha$-bungarotoxin to the 10 nM I-BTX. Binding was performed in a modified Earle's balanced salt solution (1.8 mM $CaCl_2$, 0.8 mM $MgSO_4$, 5.4 mM KCl, 116 mM NaCl, 1 mM $NaH_2PO_4$, 10 mM HEPES, 120 mM glucose, pH 7.3) supplemented with 0.2% fetal bovine serum. I-BTX binding to duplicate dishes was measured for each drug concentration in each experiment, and binding curves were measured in two to four experiments with each drug.

Standard techniques were used for whole-cell recording (10, 17) at room temperature (22–25°). The pipette (internal) solution contained 140 mM NaCl, 20 mM HEPES, 1.0 mM $MgCl_2$, and 2.0 mM EGTA, pH 7.3, 290–300 mOsm. The bath contained 140 mM NaCl, 10 mM HEPES, 0.5 mM $CaCl_2$, 20 mM glucose, pH 7.3, 310–330 mOsm, and 1 $\mu$M atropine sulfate. Drugs were applied through a multiline perfuser (18) for 5–10 sec. The time for the concentration change to be complete was ~0.5 sec in these experiments (10). A standard concentration of 40 nM ACh was applied to QF18 cells, and a concentration of 400 nM ACh was used for QA33 cells, although observations were also made at some other concentrations of ACh (see Results). Applications of ACh alone were interspersed between tests of the NDBs, and currents in response to ACh plus the NDB were normalized to the mean response to ACh alone for that cell. We found that the blocking effects of pancuronium developed slowly (see also Ref. 19), so cells were preexposed to a given concentration of pancuronium for 30 sec before the application of ACh plus pancuronium. Other drugs were applied with ACh, as preliminary experiments suggested that the block was fully developed within a few seconds.

Whole-cell responses were filtered at 20–300 Hz (eight-pole Bessel filter; Frequency Devices, Haverhill, MA) and digitized at 50–1000 Hz with a 486-based computer. The size of a response was taken as the mean value for a 1–2-sec segment when the response was stable, and base-line was taken as the mean value for segments preceding and after the response.

Data for the inhibition of the initial rate of I-BTX binding and the block of ACh-elicited current were fit using NFITS (provided by Dr. C. Lingle, Washington University School of Medicine). Estimates for the best-fitting values for the parameters of the fit equation are presented, and the 90% confidence intervals are calculated for the parameters. The values presented are the result of fitting the equations to the pooled observations for a given receptor type and drug combination, with each value given equal weight.

## Results

**Drug binding to the AChR.** We studied the ability of four NDBs to interact with muscle AChR. Binding of each NDB was determined from the inhibition of the initial rate of binding of I-BTX by various concentrations of the NDB (Fig. 1). The data were first analyzed by fitting the Hill equation

$$Y = (X/IC_{50})^n/(1 + (X/IC_{50})^n) \quad (1)$$

where $Y$ is the fractional initial rate of binding, $X$ is the drug concentration, $IC_{50}$ is the concentration of drug producing half-inhibition of binding from the Hill equation, and $n$ is the Hill coefficient. As shown in Table 1, values for the Hill coefficient were usually <1. This observation has been made previously and has been shown to result from the presence of two sites with differing affinities for the NDBs (3, 4). Accordingly, the data in Fig. 1 were also fit with an equation describing the occupation of two independent sites present in equal number:

$$Y = 0.5(X/L1)/(1 + (X/L1)) + 0.5(X/L2)/(1 + (X/L2)) \quad (2)$$

where $L1$ and $L2$ are the dissociation constants for the two independent sites. The estimates for $L1$ and $L2$ are given in Table 1, and the lines in Fig. 1 show the predicted inhibition curves for Equation 2.

**Drug effects on ACh-elicited currents.** The functional consequences of drug binding were determined with whole-cell patch-clamp recordings of membrane currents elicited by ACh in the absence and presence of the blocking drugs. The response in the presence of drug was normalized by the response of that cell to ACh in the absence of drug. We wanted to determine the consequences of drug binding to the

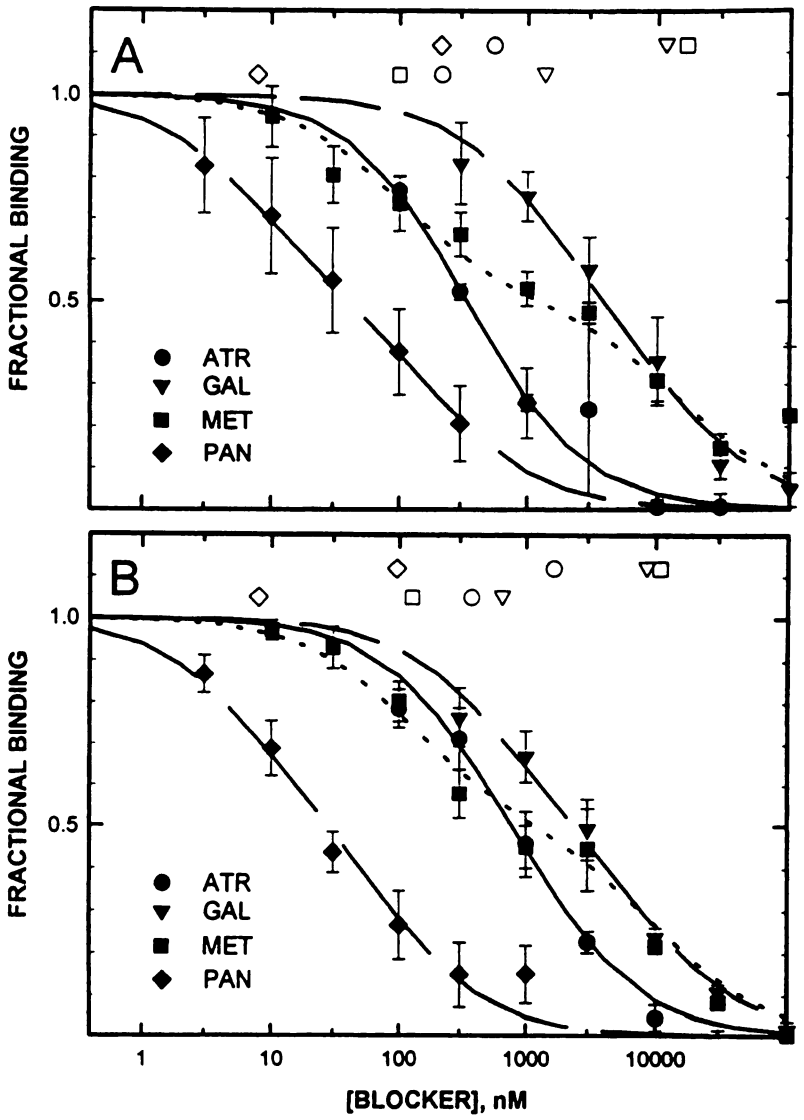


**Fig. 1.** Binding of NDBs to fetal- and adult-type AChRs. The fractional reduction produced by various concentrations of NDBs in the initial rate of I-BTX binding is shown for adult-type (QA33 cell; A) and fetal-type (QF18 cells; B) receptors. The symbols show the mean ± standard deviation of the data for two to four separate experiments with each NDB. *ATR* = atracurium, *GAL* = gallamine, *MET* = metocurine, *PAN* = pancuronium. ○, ◇, ▽, and □, Dissociation constants for the high and low affinity sites. *Lines*, curves predicted by the two-site model using the values for dissociation constants given in Table 1.

ACh-binding sites of the AChR. However, it is known that NDBs can block the open channel of the AChR (20, 21). Open-channel block is strongly voltage dependent (e.g., channel block by curare changes *e*-fold for a 30 mV membrane potential change; Ref. 20), so the effects of NDBs on ACh-elicited currents were measured at holding potentials of −50 mV and −100 mV. There was no significant difference in the mean normalized responses at −50 and −100 mV for any of the drugs for either type of AChR (data not shown; two-tailed *t* test). Furthermore, in cases in which the drugs inhibited current, the parameter estimates obtained when the Hill equation was fit to the data also did not differ between data obtained at −50 mV and at −100 mV (data not shown). We conclude that the open-channel-blocking effect of these drugs is not of major importance at these concentration ranges of ACh and drugs (see also Ref. 10 for curare). Accordingly, data obtained at −50 and −100 mV have been pooled for analysis and presentation in the figures.

The functional consequences of NDB binding are summarized in Fig. 2 (QA33 cells, adult-type receptors) and Fig. 3 (QF18 cells, fetal-type receptors). The data are shown as relative responses normalized to the current elicited from a cell by ACh applied in the absence of any NDB. As seen in Fig. 2, all of the drugs reduced the currents elicited by activation of adult-type receptors by 400 nM ACh. The concentration of NDB required to reduce the ACh-elicited current by 50% is close to the dissociation constants of the NDBs at the high affinity binding site (compare with Fig. 1), as would be expected if occupation of one site on an AChR by an NDB prevented activation when ACh occupied the second site. When the data were fit with the Hill equation, the value for the $IC_{50}$ was closer to the estimate for $L1$ than for $L2$ (see Table 1). This is the behavior expected if the NDBs act as competitive antagonists, with no partial agonist activity, and activation of the AChR occurs in large part after the binding of two ACh molecules.

The data shown in Fig. 3 show some differences between fetal- and adult-type receptors. Pancuronium and gallamine (Fig. 3A) appear to act as competitive antagonists. However, atracurium (Fig. 3B) and metocurine (Fig. 3C) are both less efficacious than expected, and some concentrations of metocurine actually enhance the response to 40 nM ACh. This second type of behavior is that expected if atracurium and

TABLE 1

**Experimental parameters for NDB binding and block of currents**

*Top*, The binding of NDBs was estimated from their ability to reduce the initial rate of I-BTX binding (Fig. 1) and analyzed by fitting the Hill equation (estimates of the $IC_{50}$ values and Hill coefficients) and a model in which two sites of different affinity were present in equal number ("two-site model"; estimates of the dissociation constants *L*1 and *L*2) (see text). The values in parentheses give the estimated 10-90% confidence limits on the fit values. QF18 cells express fetal receptors, and QA33 cells express adult receptors. Binding curves were determined on duplicate dishes in 2-4 separate experiments. For this and subsequent tables, the results are presented in terms of increasing values for the dissociation constant for the high affinity site (*L*1). *Bottom*, The ability of NDBs to reduce currents elicited by ACh were determined in voltage-clamped cells. QA33 cells were exposed to 400 nM ACh (see text), whereas QF18 cells were tested with 40 nM ACh. Inhibition curves (Figs. 2 and 3) were fit within the Hill equation;, when no value is presented, the NDB showed partial agonist activity. Predicted $IC_{50}$ was calculated assuming that an NDB acted as a competitive inhibitor with dissociation constants *L*1 and *L*2 (see text). Data were obtained from 3-10 cells. Data for curare are included for comparison (10).

| | Hill equation | | Two-site model | |
|---|---|---|---|---|
| | $IC_{50}$ | $n_H$ | *L*1 | *L*2 |
| | nM | | nM | |
| Reduction of I-BTX binding | | | | |
| QF18 | | | | |
| Pancuronium | 27 (4) | 0.73 (0.08) | 8 (3) | 95 (39) |
| Curare | 274 (44) | 0.72 (0.06) | 71 (21) | 1,116 (228) |
| Metocurine | 1,161 (270) | 0.53 (0.07) | 126 (65) | 10,788 (3409) |
| Atracurium | 792 (155) | 0.91 (0.12) | 372 (225) | 1,633 (828) |
| Gallamine | 2,375 (301) | 0.74 (0.07) | 649 (189) | 8,538 (2390) |
| QA33 | | | | |
| Pancuronium | 41 (10) | 0.63 (0.11) | 8 (3) | 210 (98) |
| Curare | 244 (30) | 0.71 (0.05) | 61 (13) | 1,027 (159) |
| Metocurine | 1,325 (563) | 0.45 (0.06) | 99 (50) | 16,451 (5291) |
| Atracurium | 343 (23) | 0.96 (0.06) | 215 (80) | 548 (214) |
| Gallamine | 3,965 (637) | 0.81 (0.10) | 1,353 (551) | 11,425 (4703) |

| | Hill equation | | Predicted $IC_{50}$ |
|---|---|---|---|
| | $IC_{50}$ | $n_H$ | |
| | nM | | nM |
| Block of ACh-elicited current | | | |
| QF18 | | | |
| Pancuronium | 5 (0.4) | 1.23 (0.14) | 7 |
| Curare | | | 64 |
| Metocurine | | | 123 |
| Atracurium | | | 270 |
| Gallamine | 1,080 (86) | 0.92 (0.07) | 571 |
| QA33 | | | |
| Pancuronium | 11 (1) | 1.06 (0.11) | 7 |
| Curare | 54 (14) | 1.02 (0.13) | 55 |
| Metocurine | 129 (11) | 0.99 (0.08) | 98 |
| Atracurium | 139 (9) | 1.24 (0.09) | 135 |
| Gallamine | 1,719 (151) | 1.05 (0.09) | 1,129 |

metocurine acted as weak partial agonists at fetal-type AChR.

**Relationship between binding and functional effects.** The data on binding of NDBs and the functional consequences were related using a kinetic scheme for the binding of ligands to the AChR and channel opening (Fig. 4). This scheme is the simplest one that incorporates the observations that there are two binding sites on each AChR and that the two sites show different affinities for ACh and for NDBs. The high and low affinity sites have dissociation constants of *K*1 and *K*2 for ACh and of *L*1 and *L*2 for NDBs, respectively. The data have been analyzed using two different assumptions: that the same site has a high affinity for both ACh and the NDBs or the site with a high affinity for NDBs has a low affinity for ACh (as shown in Fig. 4). We have assumed throughout that the high affinity site is the same for all of the NDBs (see below). The ion channel of the AChR can open (closed channel, R; open channel, R*), with a ratio of the opening to closing rates (the opening equilibrium ratio) that depends on the state of ligation of the receptor. For AChR with one bound ACh molecule, the ratio is termed R1; with two bound ACh, R3; with two molecules of an NDB bound, P3; and with one ACh and one NDB bound to the same receptor, P1. An NDB that had values for gating of P1 = 0 and P3 = 0 would not result in channel opening and would prevent activation by ACh when the NDB was bound to either site on the AChR. Such a drug would be a competitive inhibitor. An NDB would be a partial agonist if some gating occurred after binding of the NDB (P3 > 0) or for heteroliganded AChR (P1 > 0).

The predictions of this scheme were fit to the data for the effects on each NDB on ACh-elicited currents. Note that the complete scheme was used, including occupation of either site on the AChR. The values for *L*1 and *L*2 were set to those obtained in the binding experiments (Table 1). Values for ACh binding (*K*1 and *K*2) and channel gating (R1 and R3) were set to the values used in an earlier study (10; see Table 2). The model, then, was fit to the data by adjusting the values for P1 (opening of channels of AChR with ACh and one NDB bound) and P3 (opening of channels with two NDBs bound). The quality of fit was assessed visually. In the text, we present estimates for P1 based on the assumption that the site with a high affinity for NDBs has a low affinity for ACh (see also Discussion).

All of the NDBs studied seemed to act as competitive antagonists for the adult-type AChR expressed by QA33 cells, as expected from the close agreement between the values for *L*1 for binding and the $IC_{50}$ for block of ACh elicited currents (see Table 1). The curves superimposed on the data in Fig. 2 show predictions that are made using the kinetic model and setting both P1 and P3 to zero (no opening by the NDB alone or in combination with ACh). There is excellent agreement between the data and the predictions. We use 400 nM ACh as the standard test concentration for experiments with QA33 cells to ensure relatively robust control responses. However, the partial agonist activity of an NDB is most manifest at low ACh concentrations (see below and Ref. 10). In essence, if gating of heteroliganded receptors occurs, the ability of the NDB to block ACh-elicited currents will be reduced at lower ACh concentrations. Therefore, we also determined the ability of atracurium, gallamine, and metocurine to block currents elicited by 100 nM ACh, by using a concentration of the NDB near its $IC_{50}$. In each case, the block was at least as efficacious as with 400 nM ACh. In the presence of 100 nM atracurium, the current elicited by 400 nM ACh was reduced to 0.60 ± 0.08-fold the current elicited by 400 nM ACh alone (mean ± standard deviation, seven experiments), whereas 100 nM atracurium reduced the current elicited by 100 nM ACh to 0.53 ± 0.13-fold control (11 experiments). (The predicted relative current with 100 nM ACh plus 100 nM atracurium is 0.58-fold the current with 100 nM ACh alone, assuming that atracurium acts as a competitive antagonist.) Similarly, 3 μM gallamine reduced the current elicited by 400 nM ACh to 0.36 ± 0.12-fold control (nine experiments) and reduced the current elicited by 100 nM ACh to 0.15 ± 0.14-fold (five experiments), with a predicted reduction to 0.24. With 100 nM metocurine, the current elicited

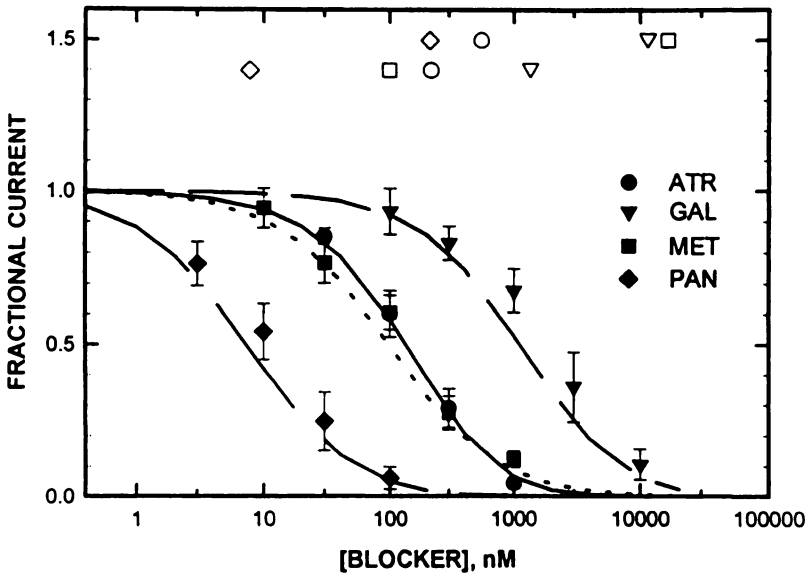


**Fig. 2.** Block of currents elicited from adult-type receptors by ACh. The current elicited by 400 nM ACh in QA33 cells in the presence of various concentrations of NDBs is shown, normalized to the current elicited in a cell by ACh alone. The half-blocking concentrations for the NDBs are shown in Table 1. *Lines*, blocking curve predicted if the NDBs acted as competitive antagonists, with dissociation constants for the high and low affinity sites on the AChR obtained from the inhibition of I-BTX binding (see text). ○, ◇, ▽, and □, Dissociation constants for the high and low affinity sites (replotted from Fig. 1A). *ATR* = atracurium, *GAL* = gallamine, *MET* = metocurine, *PAN* = pancuronium. Data are mean ± standard deviation for 3–10 experiments for each NDB.

by 400 nM ACh was reduced to 0.61 ± 0.06 (seven experiments) and by 100 nM ACh to 0.51 ± 0.17 (11 experiments), with a predicted reduction to 0.49. Gallamine reduced currents elicited by 100 nM ACh significantly more than currents elicited by 400 nM ACh ($p < 0.01$, two-tailed $t$ test), but enhanced block at lower ACh concentrations is the opposite effect of that predicted by partial agonist activity.

The block of currents elicited by ACh applied to fetal-type AChR differed between the NDBs. Block by pancuronium and gallamine could be described if it were assumed that both drugs had negligible partial agonist activity (Fig. 3A). However, the block by gallamine was somewhat less than predicted from the binding data (compare *dashed line* with ▼ in Fig. 3A). All of the data in Fig. 3A were obtained with 40 nM ACh, so we assessed the blocking ability of 3 μM gallamine on currents elicited by 400 nM ACh to determine whether the discrepancy was likely to arise from a weak partial agonist activity. Gallamine would be predicted to be more effective at blocking currents elicited by 400 nM ACh in this case, but we found that it seemed to be somewhat less effective. With 3 μM gallamine, the current elicited by 40 nM ACh was reduced to 0.28 ± 0.03-fold the current elicited by 40 nM ACh alone (eight experiments), whereas the current elicited by 400 nM ACh was reduced to 0.49 ± 0.02-fold (seven experiments), with a predicted reduction to 0.15. Therefore, there was no indication that gallamine showed significant partial agonist activity at fetal-type AChR. We have no explanation for the difference between the predicted and observed block of currents by gallamine.

Both atracurium (Fig. 3B) and metocurine (Fig. 3C) appeared to act as weak partial agonists at fetal-type receptors. In both cases, the inhibition curves predicted for a competitive antagonist with the dissociation constants obtained from the binding data lay well to the left of the data. In the case of atracurium, we could not detect measurable activation by atracurium alone (although occasional single-channel currents were seen in whole-cell recordings during the application of atracurium alone). The effect of atracurium on currents elicited by 40 nM ACh could be described by an opening equilibrium ratio for AChR with one bound ACh and one atracurium (P1) of 0.01 and setting the ratio with two atracuriums bound (P3) to 0 (Fig. 3B, *solid line*, and Table 2). We tested the ability of atracurium to block currents elicited by 400 nM ACh (Fig. 3B, ▽). With 1 μM atracurium, the current elicited by 40 nM ACh was reduced to 0.66 ± 0.23-fold control (16 experiments), whereas the current elicited by 400 nM ACh was reduced to 0.45 ± 0.14 (five experiments). The reductions in currents elicited by 40 nM and 400 nM ACh differ from each other at $0.05 < p < 0.1$ (two-tailed $t$ test). The values for P1 and P3 estimated from fitting the data obtained with 40 nM ACh gave a predicted reduction to 0.24-fold the response to 400 nM ACh alone (Fig. 3B, *dashed line*). Atracurium seems to be a weak partial agonist for fetal-type AChR.

Metocurine showed clear agonist activity. Currents could be elicited by metocurine alone when applied to QF18 cells (Fig. 3C, □), providing an estimate for P3 of $7 \times 10^{-5}$. The enhancement of currents elicited by 40 nM ACh could be described with a value for P1 of 0.72 (Table 2). Application of 1 μM metocurine was clearly more effective at blocking currents elicited by 400 nM ACh than currents elicited by 40 nM ACh (Fig. 3C, ▽). With 1 μM metocurine, the current elicited by 40 nM ACh was enhanced to 1.22 ± 0.28 (15 experiments), whereas the current elicited by 400 nM ACh was reduced to 0.29 ± 0.06 (three experiments), with a predicted reduction to 0.21 (Fig. 3C, *dashed line*). The effects of 1 μM metocurine on currents elicited by 40 nM and 400 nM ACh differ from each other at $p < 0.01$ (two-tailed $t$ test). Metocurine has clear partial agonist activity at fetal-type receptors.

**Interactions between NDBs.** Studies of the ability of NDBs to block nerve-evoked muscle twitches have shown that, in some cases, administration of a combination of two NDBs may be more effective than either one alone (22, 23). It has been suggested that a possible basis for this more-than-additive effect might be that these drugs interact differently with the two binding sites on each receptor; if the high affinity site for one drug were the low affinity site for a second, the combination might produce greater block than predicted from the effects of the individual drugs (22). We examined the interactions of gallamine and metocurine, as these drugs have been reported to show relatively robust interactions on rodent muscle (22, 23).

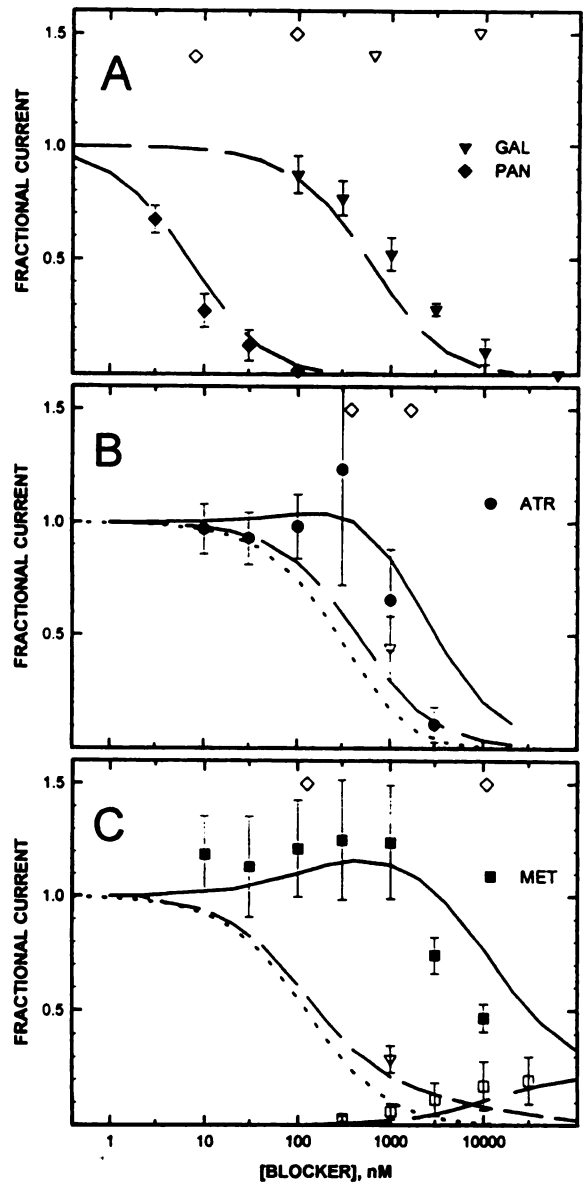


**Fig. 3.** Effects of NDBs on currents elicited from fetal-type receptors by ACh. The current elicited by 40 nM ACh in QF18 cells in the presence of various concentrations of NDBs is shown, normalized to the current elicited in a cell by ACh alone. A, Data obtained with pancuronium and gallamine. ◇ and ▽, Dissociation constants for the high and low affinity sites (replotted from Fig. 1A). *ATR* = atracurium, *GAL* = gallamine, *MET* = metocurine, *PAN* = pancuronium. *Lines*, blocking curves predicted for competitive antagonists (as in Fig. 2). These NDBs appeared to act as competitive antagonists. B, Data obtained with atracurium. There seemed to be a significant difference between the predicted blocking curve (*dotted line*) and the data (*symbols*). *Solid line*, curve predicted if atracurium acted as a weak partial agonist, with the parameters shown in Table 2. ▽, Current elicited by 400 nM ACh in the presence of 1000 nM atracurium relative to the current elicited by 400 nM ACh alone. *Dashed line*, curve predicted for block of current elicited by 400 nM ACh. C, Data obtained with metocurine. Symbols are as in B. □, Currents activated by metocurine in the absence of ACh relative to the current elicited in the same cell by 40 nM ACh. *Dashed line*, concentration-effect relationship for metocurine described by the value for P3 given in Table 2.

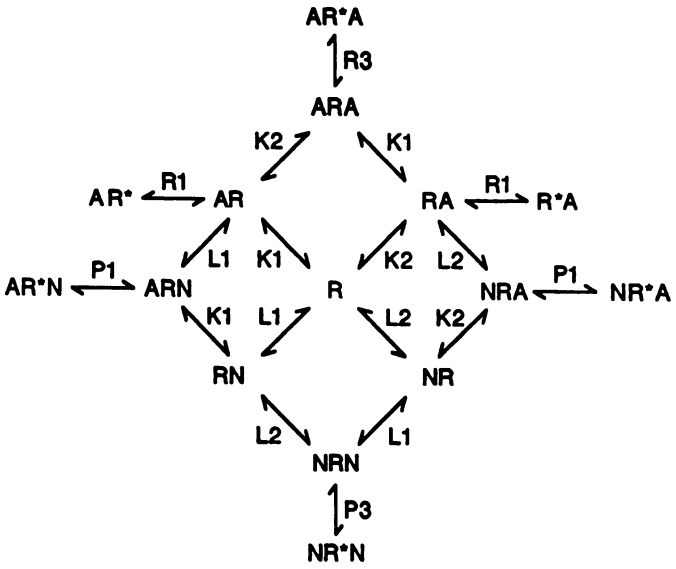


**Fig. 4.** The kinetic scheme used to analyze the interaction among ACh, NDBs, and the AChR. Each receptor (*R*) has two sites that can bind either ACh (*A*) or an NDB (*N*). As drawn, the site with the higher affinity for NDBs (dissociation constant *L*1) has the lower affinity for ACh (*K*2), and conversely. The channel of the receptor can open (R*); the equilibrium opening ratio (the ratio of the opening to the closing rates) is highest if both sites are occupied by ACh (AR*A; ratio R3 in Table 2). It is assumed that the opening ratios for the two forms of heteroliganded receptor (NR*A or AR*N) are identical (P1 in Table 2). Finally, the possibilities that channels may open with only one ACh molecule bound (AR* or R*A; ratio R1 in Table 2) or with two NDB molecules bound (NR*N; ratio P3 in Table 2) are included. As explained in the text, the parameters for ACh binding and activation were set to values used in a previously (30), and values for *L*1 and *L*2 were set to values determined from binding experiments (Table 1). The predictions of the kinetic scheme were then fit to the data by adjusting values for P1 and P3. The values obtained for P1 and P3 are presented in Table 2.

The ability of metocurine to inhibit the initial rate of I-BTX binding was measured in the presence of a concentration of gallamine able to occupy most of the high affinity binding sites for gallamine. As shown in Fig. 5A, gallamine alone reduced the initial rate by ~50%. The ability of metocurine to reduce I-BTX binding was much better described by the hypothesis that the high affinity site for gallamine is also the high affinity site for metocurine (Fig. 5A). Note that no free parameters were used to generate the predicted curves shown in this figure, as all dissociation constants were obtained from the data shown in Fig. 1 (also Table 1).

It can be difficult to assess relatively small shifts in concentration-effect curves, as would be shown by a more-than-additive inhibition curve on ACh-elicited currents. However, in the case of metocurine applied to QF18 cells, it is relatively straightforward to determine the ability of gallamine to reduce the enhancement of ACh-elicited currents produced by metocurine. The data in Fig. 5B show the ability of increasing concentrations of gallamine to reduce the currents elicited by the combination of 40 nM ACh plus 1000 nM metocurine. Again, the data are better described by the hypothesis that gallamine and metocurine have the same high affinity site on the AChR. As in Fig. 5A, no free parameters were used in generating the predicted curves, as the dissociation constants were taken from Table 1 and values for channel gating were taken from Table 2.

## Discussion

We determined the apparent affinities for four NDBs to fetal- and adult-type muscle nicotinic receptors by measuring their ability to reduce the initial rate of I-BTX binding. The

TABLE 2

**Parameters used in describing receptor activation**

The effects of NDBs on ACh-elicited currents and their ability to directly activate currents, were analyzed in terms of a two-site kinetic model (see Fig. 4 and the text). ACh binding and channel gating were described with the use of a standard set of assumed values (K1, K2, R1, and R3; see text and Ref. 30). The binding of an NDB was described with the use of the dissociation constants estimated using the two-site model from binding data (L1 and L2; see Table 1). Gating by NDBs in the absence of ACh was described assuming that channels opened only for diliganded receptors and so was described by adjusting the ratio P3. Gating of heteroliganded receptors (with one ACh and one NDB molecule bound) was characterized by the opening ratio P1. P1 was estimated for two conditions: that the NDB and ACh both bound to the same site with high affinity (Same sites) or that the site with high affinity for an NDB had a low affinity for ACh (Inverse sites). Values in parentheses give the range that produced an adequate fit (judged by eye). Data for curare are included for comparison (10).

| ACH | Binding | | Gating | | |
|---|---|---|---|---|---|
| | *K1* | *K2* | R3 | R1 | |
| | *nM* | | | | |
| QF18 | 1,000 | 500,000 | 100 | 0 | |
| QA33 | 5,000 | 500,000 | 40 | 0.0075 | |
| | *L1* | *L2* | *P3* | *P1* (same sites) | *P1* (inverse sites) |
| | *nM* | | | | |
| QA33 | | | | | |
| Pancuronium | 8 | 210 | 0 | 0 (<0.05) | 0 (<0.003) |
| Curare | 61 | 1,027 | 0 | 0 (<0.01) | 0 (<0.0001) |
| Metocurine | 99 | 16,451 | 0 | 0 (<0.2) | 0 (<0.002) |
| Atracurium | 215 | 548 | 0 | 0 (<0.01) | 0 (<0.005) |
| Gallamine | 1,353 | 11,425 | 0 | 0 (<0.02) | 0 (<0.04) |
| QF18 | | | | | |
| Pancuronium | 8 | 95 | 0 | 0 (0) | 0 (0) |
| Curare | 71 | 1,116 | 0.0003 | 0.42 (0.3–0.5) | 0.026 (0.02–0.03) |
| Metocurine | 126 | 10,788 | 0.00008 | 0.72 (0.5–0.8) | 0.01 (0.005–0.02) |
| Atracurium | 372 | 1,633 | 0 | 0.1 (0.05–0.2) | 0.01 (0.005–0.02) |
| Gallamine | 649 | 8,538 | 0 | 0 (<0.04) | 0 (<0.04) |

assays were performed in intact cells (to avoid possible effects of detergents on affinities) and in a system in which mixing is rapid. In the same preparation of cells, we recorded voltage-clamped membrane currents to examine the abilities of these drugs to activate currents or to affect the ability of ACh to elicit currents. We find that all drugs, as expected, show evidence for the existence of two sites with different affinities on each AChR. The rank order of affinities is identical for both fetal- and adult-type receptors. The affinities estimated from binding experiments can be used to describe the concentration dependence of functional effects, either block or activation, by the NDBs. We also find that at least two of the NDBs (gallamine and metocurine) share the same high and low affinity sites on each receptor.

The clinically desired effect of NDBs is to block nerve-evoked muscle contractions. Unfortunately, there are few data on mouse muscles, but Table 3 summarizes data obtained from studies of indirect twitches evoked in rat or guinea pig muscles studied in organ baths (in which problems of drug binding and distribution should be reduced). The concentrations needed to produce half-block of twitch are higher than the dissociation constants we have obtained for NDB binding to the high affinity site on adult-type receptors (*L*1; see Table 1). This divergence is expected because block of twitch requires that >90% of the receptors have NDB bound to at least one site (for a discussion, see Ref. 1). In the cases of atracurium, gallamine, and curare, the half-blocking concentrations are ~20-fold higher than *L*1, but the order of potency is the same for blocking twitch and for binding to the high affinity site. The most disparate value is that for pancuronium, which is much less effective at blocking twitches than expected. The reason for this difference is not known, but the general agreement is as would be expected if the major determinant of the clinical actions of NDBs was competitive inhibition of ACh binding and activation.

The apparent affinities we estimated for the high and low affinity binding sites on fetal-type receptors are in agreement with a number of previous studies, as indicated by the comparisons in Table 4. Fewer studies have been made of functional consequences of NDB binding, but these studies are in general agreement with our results (Table 4).

In comparing the actions of these drugs on fetal- and adult-type receptors, we found that they share the same rank order for affinities for binding at the high affinity site (*L*1 in Table 1) and, except for atracurium and curare, at the low affinity site. Our estimates for dissociation constants show some quantitative differences in comparing data from adult- and fetal-type receptors, but the differences are generally <1.5-fold. The differences are greatest for atracurium (in *L*2) and gallamine (in *L*1). There is no indication of a major systematic difference in affinities at the high affinity site (where the adult-type receptor has an $\epsilon$ and the fetal-type receptor has a $\gamma$ subunit; see discussion below).

A number of studies have shown that the site that has higher affinity for curare (6, 24) or metocurine, pancuronium, and gallamine (25) is located at the $\alpha\gamma$ interface. Similarly, curare has a high affinity at the site formed at the $\alpha\epsilon$ interface (26). Conversely, curare (5, 24) and metocurine (27) have a low affinity for the site at the $\alpha\delta$ interface. In this light, it is perhaps surprising that the high affinity sites on fetal- and adult-type mouse receptors have such similar dissociation constants. Sine (7) mapped the residues that determine the difference in affinity between mouse $\gamma$ and $\delta$ subunits; in the $\gamma$ subunit, $Ile^{116}$, $Tyr^{117}$, and $Ser^{161}$ contribute to the high affinity, whereas $\delta$ subunit has $Val^{118}$, $Thr^{119}$, and $Lys^{163}$ in the homologous positions. A conversion of $Tyr^{117}$ to threonine in the $\gamma$ subunit resulted in a 10-fold increase in the value for *L*1 for metocurine, whereas the conversion of $Lys^{163}$ to serine in the $\delta$ subunit resulted in a 4-fold decrease in *L*1. Surprisingly, the $\epsilon$ subunit has $Val^{116}$, $Ser^{117}$, and $Ala^{161}$ in the

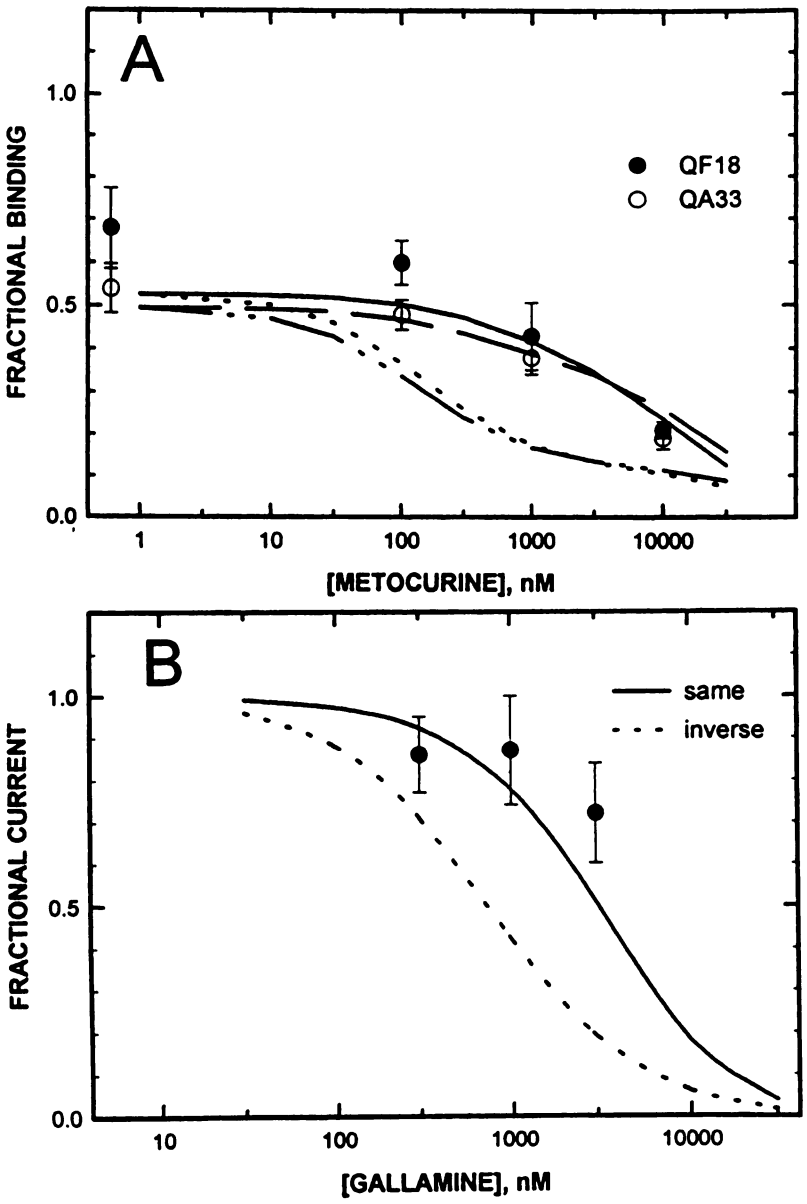


**Fig. 5.** Interactions between two NDBs at sites on the AChR. Interactions between gallamine and metocurine were examined on both adult- and fetal-type receptors. A, Effect of a constant concentration of gallamine on the ability of increasing concentrations of metocurine to reduce the initial rate of I-BTX binding. QA33 cells were exposed to 4000 nM gallamine, and QF18 cells were exposed to 2000 nM gallamine, in the presence of 0, 100, 1,000, or 10,000 nM metocurine. *Left*, data obtained with 0 nM metocurine. *Curves*, predicted reductions in the initial rates assuming that metocurine and gallamine share the same high affinity site (*solid line*, fetal-type receptors; *dashed line*, adult-type receptors) or have inverted affinities (*dotted line*, fetal-type receptors; *dashed/dotted line*, adult-type receptors). The curves were generated with the values for $L1$ and $L2$ shown in Table 1 (no parameters were adjusted). The agreement between prediction and observation is very good for data from QA33 cells. The predicted curve for data from QF18 cells lies below the observations. The prediction is much closer if a value of 1300 nM is used for $L1$ rather than 649 nM (Table 1). B, Ability of increasing concentrations of gallamine to block the potentiated current produced by the application of 40 nM ACh plus 1000 nM metocurine to fetal-type receptors. The current has been normalized to the potentiated current produced in the absence of gallamine. The curves are predicted with the values for activation shown in Table 2 for the case that metocurine and gallamine have the same high affinity site (*solid line*) or inverted sites (*dotted line*). No parameters were adjusted in making the predictions.

TABLE 3

**Concentrations of NDBs required to block twitches**

The concentrations of various drugs required to reduce by 50% the amplitude of the nerve-evoked twitch in rat or guinea pig muscles. All data were obtained with excised muscles. The reference for the value is given in parentheses. Ratio presents the ratio of the mean $IC_{50}$ to the value for L1 obtained from binding to adult receptors (Table 1, *top*).

| | Pancuronium | Curare | Atracurium | Gallamine |
|---|---|---|---|---|
| | 2,442 (29) | 1,437 (30) | 800 (31) | 30,000 (32) |
| | 2,700 (33) | 1,000 (33) | 11,200 (34) | 3,090 (35) |
| | 1,100 (32) | 391 (36) | | |
| | | 600 (36) | | |
| | | 6,700 (32) | | |
| | | 349 (35) | | |
| Mean | 2,081 | 1,746 | 6,000 | 16,545 |
| Ratio | 260 | 29 | 28 | 12 |

homologous positions, residues which are more similar to those of the δ subunit. The possibility exists that compensating differences exist elsewhere; for example, the ε subunit has a tyrosine residue at position 124, whereas both γ and δ have a phenylalanine residue in the homologous position. Further analyses will be required to resolve this question.

These previous results also suggest that all NDBs have the same high affinity site for fetal-type receptors. A number of reports have been made, however, that combinations of two NDBs may show a positive interaction in blocking twitches (compare with Ref. 22). It has been suggested that a possible explanation for this interaction is that the high affinity site for one NDB is the low affinity site for the other, so that the combined application would occupy a larger proportion of the free sites on AChRs than predicted if they competed at the same sites (22). We directly examined the interaction of gallamine and metocurine at both fetal- and adult-type receptors. Gallamine and metocurine were chosen because they showed a relatively large interaction in studies on guinea pig muscle (22, 23) and because the large separations of $L1$ and $L2$ facilitated the analysis. Furthermore, the fact that metocurine acted as a partial agonist at fetal-type receptors meant that we could examine the ability of gallamine to block functional effects of metocurine on fetal-type receptors. All of

TABLE 4

**Other estimates of dissociation constants for NDB binding to mouse muscle receptors**

Several studies have determined dissociation constants for NDB binding to the high and low affinity sites on mouse muscle receptors through analysis of the ability of NDBs to reduce the initial rate of I-BTX binding to cells expressing various mouse muscle receptor subunits (values for L1 and L2). Fewer studies have estimated $IC_{50}$ values or apparent dissociation constants for inhibition of agonist-elicited flux or voltage-clamped membrane current. The first column shows the subunit composition studied, and the reference for the values is given in parentheses.

| | Pancuronium | | Curare | | Metocurine | | Gallamine | |
|---|---|---|---|---|---|---|---|---|
| | *L1* | *L2* | *L1* | *L2* | *L1* | *L2* | *L1* | *L2* |
| | | | | | *nM* | | | |
| Inhibition of I-BTX binding | | | | | | | | |
| $\alpha, \beta, \gamma, \delta$ | | | | | 180 | 8,500 | | (37) |
| $\alpha, \beta, \gamma$ | 12 | | | | 200 | | 1,500 | (25) |
| $\alpha, \beta, \gamma, \delta$ | | | | | 180 | 4,900 | | (7) |
| $\alpha, \beta, \gamma, \delta$ | 9.1 | 69 | | | 309 | 27,500 | 3,700 | 55,000 (3) |
| $\alpha, \beta, \gamma, \delta$ | | | | | 84 | 6,100 | | (35) |
| $\alpha, \beta, \gamma$ | | | | | 106 | | | (27) |
| $\alpha, \beta, \delta$ | | | | | | 3,700 | | (27) |
| $\alpha, \beta, \gamma, \delta$ | | | 56 | 1,600 | | | | (11) |
| $\alpha, \beta, \epsilon, \delta$ | | | 56 | 1,600 | | | | (11) |
| Mean | 11 | 69 | 56 | 1,600 | 177 | 10,140 | 2,600 | 55,000 |
| | $IC_{50}$ | | $IC_{50}$ | | $IC_{50}$ | | $IC_{50}$ | |
| Inhibition of flux or current | | | | | | | | |
| $\alpha, \beta, \gamma, \delta$ | 0.9 | | 14.2 | | | | 390 | (39) |
| $\alpha, \beta, \gamma, \delta$ | 7.4 | | | | 470 | | 3,700 | (3) |

our data indicate that these two agents have the same high affinity site.

The qualitative difference in the actions of NDBs at fetal- and adult-type receptors is the finding that several have detectable partial agonist activity at fetal-type receptors, but none had any agonist activity at adult-type receptors. Two aspects of this observation will be considered. The first is the nature of the binding sites involved. The second is the structure of the NDBs that act as partial agonists.

The ability of the NDBs to potentiate or block ACh-elicited currents is seen when the high affinity site is occupied [i.e., the site at the $\alpha\gamma$ or $\alpha\epsilon$ interface (see discussion above)]. Therefore, the partial agonist activity must be associated with a difference in the interactions of NDBs with the $\alpha\gamma$ and $\alpha\epsilon$ subunit pairs. Direct gating can occur when both $\alpha\gamma$ and $\alpha\delta$ sites are occupied by some NDBs, so to a first approximation the consequences of binding to the $\alpha\delta$ site are similar to those occurring after binding to the $\alpha\gamma$ site. Therefore, even though the affinities of the NDBs we have examined are similar for the $\alpha\gamma$ and $\alpha\epsilon$ sites and different for the $\alpha\delta$ site, the resulting conformational changes are more similar for the $\gamma$ and $\delta$ subunits.

We analyzed the potentiation of ACh-elicited currents under two assumptions: that the same site on the AChR has a high affinity for ACh and for NDBs or that one site has a high affinity for ACh and a low affinity for NDBs. (Note that only the gating properties of heteroliganded receptors, described by P1 in Table 2, are affected by this.) Some biochemical data suggest that $\alpha\delta$ dimers have a higher affinity for ACh than $\alpha\gamma$ dimers (6), which suggests that the site with a higher affinity for NDBs has a lower affinity for ACh. Recent experiments with $\alpha\beta\gamma$ and $\alpha\beta\delta$ subunit combinations expressed in human embryonic kidney 293 cells suggest that gating by ACh occurs at lower concentrations with the $\alpha\beta\delta$ combination than the $\alpha\beta\gamma$ combination,[1] which would also be consistent with the idea that binding of NDBs and ACh occurs with inverted affinities at the two sites. In either case, the heteroliganded receptors have a much lower probability of opening than do receptors diliganded by ACh.

The parent NDB, curare, and its methylated derivative, metocurine, show the largest values for P1 and P3. Both have two positively charged sites in a rigid molecular structure, but this is clearly not required for partial agonist activity because the steroid derivative pancuronium has no detectable activity. Atracurium has two positively charged sites, separated by a chain with more flexibility than pancuronium, so it is possible that it can adopt a conformation more like that of curare. Gallamine is a relatively smaller molecule, with the greatest similarity to ACh, so it was somewhat surprising that it showed no detectable partial agonist activity. These data cannot provide a picture of the interactions associated with partial agonist activity but suggest that it does not depend exclusively on binding of charged groups or on the presence of an extended rigid molecule.

A recent study (28) found that some neuronal nicotinic receptor subunit combinations show similar divergence in action of curare. Rat $\alpha 2$ or $\alpha 3$ subunits, when expressed in *Xenopus* oocytes with rat $\beta 2$ subunits, produce receptors in which ACh-elicited currents are competitively inhibited by curare. In contrast, when expressed with $\beta 4$ subunits, curare could potentiate ACh-elicited currents (although no direct gating was seen). The authors analyzed their data in terms of channel opening for heteroliganded receptors but were not able to estimate relative channel opening probabilities for heteroliganded receptors compared with ACh diliganded receptors.

In sum, our data demonstrate that each of these NDBs binds to two sites on both fetal- and adult-type muscle nicotinic AChRs, with differing affinities for the two sites. Binding of NDBs was similar to the two types of receptor, with only relatively small (<3-fold) possible differences in apparent affinities for either the high or low affinity sites on the two types of receptors. The NDBs appear to share the same high and low affinity sites on both adult- and fetal-type

[1] J. H. Steinbach and K. Burris, unpublished observations.

receptors. The ability of NDBs to block ACh-elicited currents can be accounted for by binding to their high affinity site on the muscle nicotinic AChR. Only some of the NDBs show partial agonist activity for fetal-type receptors, and none showed detectable agonist activity for adult-type receptors. Our results confirm that the major clinical effects of several structurally diverse NDBs can be associated with their ability to bind to the ACh-binding sites on muscle nicotinic AChRs and prevent binding of ACh.

**Acknowledgments**

We thank Qing Chen for growing and immunopurifying all of the cells used in these experiments. We thank Steve Sine for the gift of metocurine, and Burroughs-Wellcome for the gift of atracurium.

**References**

1. Lingle, C. J., and J. H. Steinbach. Neuromuscular blocking agents. *Int. Anesthesiol. Clin.* **26**:288–301 (1988).
2. Lingle, C., D. Maconochie, and J. H. Steinbach. Activation of skeletal muscle nicotinic acetylcholine receptors. *J. Membr. Biol.* **126**:195–217 (1992).
3. Sine, S. M., and P. Taylor. Relationship between reversible antagonist occupancy and the functional capacity of the acetylcholine receptor. *J. Biol. Chem.* **256**:6692–6699 (1981).
4. Neubig, R., and J. B. Cohen. Equilibrium binding of $^3$H-tubocurarine and $^3$H-acetylcholine by Torpedo postsynaptic membranes: stoichiometry and ligand interactions. *Biochemistry* **18**:5464–5475 (1980).
5. Chiara, D. C., and J. B. Cohen. Identification of amino acids contributing to high and low affinity D-tubocurarine (dTC) sites on the Torpedo nicotinic acetylcholine receptor (nAChR) subunits. *Biophys. J.* **61**:A106 (1992).
6. Blount, P., and J. P. Merlie. Molecular basis of the two nonequivalent ligand binding sites of the muscle nicotinic acetylcholine receptor. *Neuron* **3**:349–357 (1989).
7. Sine, S. M. Molecular dissection of subunit interfaces in the acetylcholine receptor: identification of residues that determine curare selectivity. *Proc. Natl. Acad. Sci. USA* **90**:9436–9440 (1993).
8. Ziskind, L., and M. J. Dennis. Depolarising effect of curare on embryonic rat muscles. *Nature (Lond.)* **276**:622–623 (1978).
9. Kopta, C., and J. H. Steinbach. Comparison of mammalian adult and fetal nicotinic acetylcholine receptors stably expressed in fibroblasts. *J. Neurosci.* **14**:3922–3933 (1994).
10. Steinbach, J. H., and Q. Chen. Antagonist, and partial agonist actions of d-tubocurarine at mammalian muscle acetylcholine receptors. *J. Neurosci.* **15**:230–240 (1995).
11. Gu, Y., A. Franco, P. D. Gardner, J. B. Lansman, and J. R. Hall. Properties of embryonic and adult muscle acetylcholine receptors transiently expressed COS cells. *Neuron* **5**:147–157 (1990).
12. Vogel, Z., A. J. Sytkowski, and M. W. Nirenberg. Acetylcholine receptors of muscle grown *in vitro*. *Proc. Natl. Acad. Sci. USA* **69**:3180–3184 (1972).
13. Phillips, W. D., C. Kopta, P. Blount, P. D. Gardner, J. H. Steinbach, and J. P. Merlie. Acetylcholine receptor-rich membrane domains organized in fibroblasts by recombinant 43-kD protein. *Science (Washington D. C.)* **251**:568–570 (1991).
14. Tzartos, S. J., D. E. Rand, B. L. Einarson, and J. M. Lindstrom. Mapping of surface structures of Electrophorus acetylcholine receptor using monoclonal antibodies. *J. Biol. Chem.* **256**:8635–8645 (1981).
15. Chen, Q., G. H. Fletcher, and J. H. Steinbach. Selection of stably transfected cells expressing a high level of fetal muscle nicotinic receptors. *J. Neurosci. Res.* **40**:606–612 (1995).
16. Sine, S. M., and P. Taylor. Functional consequences of agonist-mediated state transitions in the cholinergic receptor. *J. Biol. Chem.* **254**:3315–3325 (1979).
17. Hamill, O. P., A. Marty, E. Neher, B. Sakmann, and F. J. Sigworth. Improved patch-clamp techniques for high-resolution current recording from cells and cell-free membrane patches. *Pfluegers Arch.* **391**:85–100 (1981).
18. Konnerth, A., H. D. Lux, and M. Morad. Proton-induced transformation of calcium channel in chick dorsal root ganglion cells. *J. Physiol.* **386**:603–633 (1987).
19. Glavinovic, M. I., M. J. C. Law, L. Kapural, F. Donati, and D. R. Bevan. Speed of action of various muscle relaxants at the neuromuscular junction binding *vs.* buffering hypothesis. *J. Pharmacol. Exp. Ther.* **265**:1181–1186 (1993).
20. Colquhoun, D., F. Dreyer, and R. E. Sheridan. The actions of tubocurarine at the frog neuromuscular junction. *J. Physiol.* **293**:247–284 (1979).
21. Sine, S. M., and J. H. Steinbach. Acetylcholine receptor activation by a site-selective ligand: nature of brief open and closed states in BC3H-1 cells. *J. Physiol.* **370**:357–379 (1986).
22. Waud, B. E., and D. R. Waud. Quantitative examination of the interaction of competitive neuromuscular blocking agents on the indirectly elicited muscle twitch. *Anesthesiology* **61**:420–427 (1984).
23. Waud, B. E., and D. R. Waud. Interaction among agents that block endplate depolarization competitively. *Anesthesiology* **63**:4–15 (1985).
24. Pedersen, S. E., and J. B. Cohen. d-Tubocurarine binding sites are located at $\alpha$-$\gamma$ and $\alpha$-$\delta$ subunit interfaces of the nicotinic acetylcholine receptor. *Proc. Natl. Acad. Sci. USA* **87**:2785–2789 (1990).
25. Fu, D. X., and S. M. Sine. Competitive antagonists bridge the $\alpha$-$\gamma$ subunit interface of the acetylcholine receptor through quaternary ammonium-aromatic interactions. *J. Biol. Chem.* **269**:26152–26157 (1994).
26. Blount, P., and J. P. Merlie. Characterization of an adult muscle acetylcholine receptor subunit by expression in fibroblasts. *J. Biol. Chem.* **266**: 14692–14696 (1991).
27. Sine, S. M., and T. Claudio. $\gamma$- And $\delta$-subunits regulate the affinity and the cooperativity of ligand binding to the acetylcholine receptor. *J. Biol. Chem.* **266**:19369–19377 (1991).
28. Cachelin, A. B., and G. Rust. Unusual pharmacology of (+)-tubocurarine with rat neuronal nicotinic acetylcholine receptors containing $\beta$4 subunits. *Mol. Pharmacol.* **46**:1168–1174 (1994).
29. Fragen, R. J., L. H. Booij, F. van der Pol, E. N. Robertson, and J. F. Crul. Interactions of diisopropyl phenol (ICI 35868) with suxamethonium, vecuronium and pancuronium *in vitro*. *British Journal of Anaesthesia* **55**:433–436 (1983).
30. Strahan, S. K., B. J. Pleuvry, and C. Y. Modla. Effect of meptazinol on neuromuscular transmission in the isolated rat phrenic nerve-diaphragm preparation. *British Journal of Anaesthesia* **57**:1095–1099 (1985).
31. Wali, F. A., A. H. Suer, C. H. Dark, and A. C. Tugwell. Assessment of neuromuscular blockade produced by atracurium in the rat diaphragm preparation. Measurements of tetanic fade, depression and recovery profile. *Pharmacological Research* **21**:231–238 (1989).
32. Birmingham, A. T., and S. Z. Hussain. A comparison of the skeletal neuromuscular and autonomic ganglion-blocking potencies of five non-depolarizing relaxants. *British Journal of Pharmacology* **70**:501–506 (1980).
33. Pollard, B. J., and R. M. Jones. Interactions between tubocurarine, pancuronium and alcuronium demonstrated in the rat phrenic nerve-hemidiaphragm preparation. *British Journal of Anaesthesia* **55**:1127–1131 (1983).
34. van der Spek, A. F., J. T. Zupan, B. J. Pollard, and M. A. Schork. Interactions of vecuronium and atracurium in an *in vitro* nerve-muscle preparation. *Anesthesia and Analgesia* **67**:240–246 (1988).
35. Lu, T. C. Affinity of curare-like compounds and their potency in blocking neuromuscular transmission. *Journal of Pharmacology & Experimental Therapeutics* **174**:560–566 (1970).
36. Waud, B. E., and D. R. Waud. Tubocurarine sensitivity of the diaphragm after limb immobilization. *Anesthesia and Analgesia* **65**:493–495 (1986).
37. Sine, S. M., P. Quiram, F. Papanikolaou, H. J. Kreienkamp, and P. Taylor. Conserved tyrosines in the $\alpha$ subunit of the nicotinic acetylcholine receptor stabilize quaternary ammonium groups of agonists and curariform antagonists. *Journal of Biological Chemistry* **269**:8808–8816 (1994).
38. Sine, S. M., and T. Claudio. Stable expression of the mouse nicotinic acetylcholine receptor in mouse fibroblasts. *Journal of Biological Chemistry* **266**:13679–13689 (1991).
39. Filatov, G. N., M. L. Aylwin, and M. M. White. Selective enhancement of the interaction of curare with the nicotinic acetylcholine receptor. *Molecular Pharmacology* **44**:237–241 (1993).

**Send reprint requests to:** Dr. Joe Henry Steinbach, Department of Anesthesiology, Washington University School of Medicine, 660 South Euclid, St. Louis MO 63110. E-mail: jhs@morpheus.wustl.edu